International Journal of Biological Macromolecules 113 (2018) 1214–1220

Contents lists available at ScienceDirect

International Journal of Biological Macromolecules

journal homepage: http://www.elsevier.com/locate/ijbiomac

Inhibition of protein kinase A affects *Paracoccidioides lutzii* dimorphism

Sheila J. Sestari [a], Wesley A. Brito [a,b,c], Bruno J. Neves [c], Celia M.A. Soares [a], Silvia M. Salem-Izacc [a,*]

[a] Laboratório de Biologia Molecular, Instituto de Ciências Biológicas, Universidade Federal de Goiás, Brazil
[b] Unidade Universitária de Ciências Exatas e Tecnológicas, Universidade Estadual de Goiás, Brazil
[c] Centro Universitário de Anápolis, UniEvangélica, Brazil

ARTICLE INFO

Article history:
Received 7 August 2017
Received in revised form 16 February 2018
Accepted 5 March 2018
Available online 6 March 2018

Keywords:
Paracoccidioides lutzii
PKA
H89

ABSTRACT

A critical step in the lifecycle of many fungal pathogens is the ability to switch between filamentous and yeast growth, a process known as dimorphism. cAMP-dependent protein kinase (PKA) controls morphological changes and the pathogenicity of several animal and plant pathogenic fungi. In this work, we report the analysis of PKA activity during the mycelium to yeast transition in the pathogenic fungus *Paracoccidioides lutzii*. This fungus, as well as the closely related species *Paracoccidioides brasiliensis*, causes paracoccidioidomycosis, a systemic mycosis that affects thousands of people in Latin America. Infection occurs when hypha fragments or spores released from mycelium are inhaled by the host, an event that triggers the morphological switch. We show here that PKA activity is regulated in the fungus phase, increasing during the mycelium to yeast transition. Also, morphological transition from mycelium to yeast is blocked by the compound H89, a specific PKA inhibitor. Nevertheless, the fungus recovers its ability to change morphology when H89 is removed from the culture media. This recovery is accompanied by a significant increase in PKA activity. Our results strongly indicate that PKA directly affects phase transition in *P. lutzii*.

1. Introduction

Protein kinases are enzymes that catalyze the transfer of a γ-phosphate group of adenosine 5′-triphosphate (ATP) to the amino acid side chains of target proteins [1–3]. They are considered the largest family of proteins in eukaryotes and play important roles in cell growth and metabolism, signal transduction, cytoskeleton rearrangement, cell division, DNA replication and transcriptional control [4,5].

The cAMP dependent protein kinase (PKA) was the first kinase to have its structure completely determined [6]. PKA is an inactive tetramer composed of two regulatory and two catalytic subunits. Its activity is modulated by changes in cAMP levels. When cAMP levels are high, it binds to the regulatory subunits of PKA, releasing the catalytic subunits that become active, subsequently phosphorylating protein kinases, transcription factors, and other substrates to control several physiological processes [7,8]. This signal transduction pathway allows organisms to rapidly respond to environmental changes.

The cAMP/PKA pathway controls morphological changes and pathogenicity in several pathogenic fungi of plants and animals, such as *Candida albicans* [9,10], *Cryptococcus neoformans* [11], *Aspergillus fumigatus* [12], *Ustilago maydis* [13,14] and *Magnaporthe grisea* [15,16]. This pathway has been extensively studied in the model organism *Saccharomyces cerevisiae*, being associated with cell growth, metabolism and resistance to stress. In *S. cerevisiae*, the regulatory subunits are encoded by the Bcy1 gene, while the catalytic subunits are encoded by three related genes, namely Tpk1, Tpk2 and Tpk3. These isoforms are functionally redundant with regard to cell viability, but they regulate different processes in the cell [17]. For example, Tpk2 is responsible for stimulating pseudohyfal morphogenesis. Its targets include the Flo8 transcription factor, which is required for the expression of Flo11 that, in turn, is responsible for promoting the adhesion of the daughter-mother cells; an event required for the growth of pseudohyphas [18]. On the other hand, Tpk1 and Tpk3 have a repressor effect in this process [19,20].

Fungi of the *Paracoccidioides* genus are the causative agent of paracoccidioidomycosis (PCM), a systemic mycosis that extends throughout Latin America. This genus comprises two closely related species: *P. brasiliensis* and *P. lutzii*, which until recently were considered a single species. The ability to change between filamentous growth and yeast is critical to the life cycle of these fungi, and important for the infection process, since strains that are unable to differentiate are often avirulent [21,22]. The infection occurs through inhalation of conidia produced by mycelium, which differentiates into yeasts in the host lungs [23]. PKA also plays an important role in *Paracoccidioides brasiliensis* dimorphic transition. It has been demonstrated that the cAMP levels increase during the mycelial to yeast transition and that dimorphism can be modulated by exogenous cAMP [24,25]. Moreover, recent studies indicate that during cAMP-controlled differentiation, there

* Corresponding author at: Lab. Biologia Molecular, Departamento de Bioquímica e Biologia Molecular, Instituto de Ciências Biológicas II, Campus Samambaia s/n, Universidade Federal de Goiás, 74690-900 Goiânia, Goiás, Brazil.
E-mail addresses: silviaizacc@gmail.com, silviaizacc@ufg.br (S.M. Salem-Izacc).

https://doi.org/10.1016/j.ijbiomac.2018.03.023
0141-8130/

is a change in the expression of Gβ-protein PbGpb1, which interacts with adenylate cyclase during the morphological transition. *In vitro* analysis showed that Gβ-PbGpb1 reduces the activity of Tpk2, suggesting that this inhibition reduces the level of expression of Flo11, which is responsible for the filamentous growth of cells. In contrast, the TupA regulatory protein, together with the Flo8 transcription factor, controls the expression of Flo11 and induces filamentous growth. Therefore, Gβ-PbGpb1 and TupA bind to Tpk2 to act as antagonistic molecular switches of cell morphology, with TupA and Gβ-PbGpb1 inducing and repressing filamentous growth, respectively [26].

In *Paracoccidioides* spp., there is a single gene coding for the regulatory subunit of PKA and the catalytic subunits are encoded by two genes, namely PbTpk1 and PbTpk2, according to the similarity with the genes of *S. cerevisiae*. These subunits have different subcellular localization. It has been demonstrated that PbTpk2 goes to the nucleus, while PbTpk1 is localized within distinct structures within the cytoplasm, indicating that they match different targets and regulate distinct processes [26].

In this work, we show that the activity of PKA is phase regulated and that this protein is essential for the mycelium to yeast transition in *P. lutzii*, since inhibition of the activity of this protein by H89, a PKA specific inhibitor, blocks the differentiation process.

2. Material and methods

2.1. Homology modeling

The amino acid sequence of *P. lutzii* PKA (accession number PAAG_04050) was retrieved from the UniProt database [27] and used as a target for homology modeling in the SWISS-MODEL server [28,29]. Subsequently, the built models were exported to the GalaxyWEB server [30], which refines loop or terminus regions by *ab initio* modeling. Finally, the structural reliability of the built models was evaluated by using MolProbity server [31], and the model with the lowest Clashscore and MolProbity score was selected for further analysis.

2.2. Computational fragment mapping calculations

Computational fragment mapping calculations were performed using the FTMap server [32,33] to identify small molecule binding hot spots in the PKA homology model. The program docks sixteen small organic molecules to determine energetically favorable binding regions.

2.3. Molecular docking

The structure of H89 was imported to Maestro workspace v.9.3 and prepared using LigPrep 2.5 (Schrödinger, LCC, New York, 2012) at pH of 7.0 ± 1.0. Subsequently, 2000 conformations were generated using OMEGA v.2.5.1 [34,35], while AM1-BCC charges [36] were added using QUACPAC v.1.6.3 [37]. At the same time the 3D structure of *P. lutzii* PKA was pre-processed using Protein Preparation Wizard available on Maestro workspace (Schrödinger LLC). During protein preparation, hydrogen atoms were first added to the proteins, and bond orders and formal charges were adjusted. The protonation state of polar amino acids was predicted by PROPKA v.3.1 (Schrödinger LLC) [38] at pH of 7.0 ± 1.0. Subsequently, full-atom protein structure minimization using the OPLS-2005 force field was carried out [39]. Prior to docking studies, a grid with the dimensions of 21.3 Å × 16.6 Å × 16.3 Å (*x*, *y*, and *z*) and volume of 5807 $Å^3$ was defined to include the full ATP-binding site of PKA. Lastly, molecular docking studies were performed using the high-resolution protocol from the FRED program and the ChemGauss4 score function, both available on OEDocking suite v.3.2.0 [40–42].

2.4. P. lutzii growth conditions and induction of phase transition in the absence and in the presence of H89

P. lutzii strain Pb01 (ATCC MYA-826) was used in our experiments. Mycelium was grown in semi-solid Fava Netto's medium (0.3% proteose peptone, 1% peptone, 0.5% meat extract, 0.5% yeast extract, 4% glucose, 0.5% NaCl and 1.4% agar, pH 7.2) at 22 °C. The mycelium to yeast transition was performed in 10 mL of liquid Fava Netto's medium by raising the incubation temperature from 22° to 36 °C. Before changing the incubation temperature, the cells were adapted in the liquid medium for 48 h under continuous agitation. After this time, the cells were harvested by centrifugation and 0.2 g of dry weighed cell mass was inoculated into fresh liquid medium, either in the absence or in the presence of different concentrations of H89 (*Sigma-Aldrich*, St. Louis, MO, USA). H89 was dissolved in water (5 mg/mL) and then used in the final concentrations of 25 μM, 50 μM and 100 μM in 10 mL of culture medium. Cells were collected at 14 h, 22 h, 48 h and 72 h for achievement of protein extracts used in the activity assays, and for the morphological analysis of phase transition. All the experiments were done in triplicate.

2.5. Recovery assay

Cells were cultured as described in Item 2.4. After 48 h of morphological transition, H89 treated cells were washed three times with phosphate buffered saline (PBS) to remove the inhibitor, and then transferred to fresh liquid Fava Netto's medium without inhibitor and grown for an additional 48 h. Altogether, cell differentiation was accompanied for 96 h.

2.6. Morphological analysis and cell viability assay of the mycelium to yeast transition

Morphological transition was accompanied under light microscopy. The mycelium to yeast transition was quantified in a Neubauer Chamber by counting the number of yeast cells that appeared in the culture medium after changing the incubation temperature from 22 °C to 36 °C. For counting, 10 μL of the cell culture was added to 190 μL trypan blue solution and diluted in PBS to a final volume of 1 mL. The solution containing the cells was vigorously shaken before being placed in the Neubauer chamber to avoid yeast lumps. Cell viability was determined using trypan blue staining and standard cell count techniques in a Neubauer chamber. Statistical comparisons were performed using Student's *t*-test, and samples with *p*-values ≤0.05 were considered statistically significant.

2.7. Protein extraction

Cells were collected by centrifugation at 2000 *g* for 10 min. Afterwards, cells were resuspended in Tris-Ca buffer (20 mM Tris-HCl, pH 8.8; 2 mM $CaCl_2$) and treated with 5 μL/mL of Protease Inhibitor Mix (GE Healthcare Life Sciences, Little Chalfont, UK). Cells were disrupted in the presence of glass beads (0.5 mm in diameter) in a mini-beadbeater apparatus (BioSpec, Oklahoma, USA) for five cycles of 30 s with 30 s cooling intervals on ice, followed by repeated centrifugation until no pellet formation was observed. Protein extracts were quantified by the Bradford method, analyzed by SDS-PAGE and used in the PKA activity assays.

2.8. Activity assays

The activity of PKA in *P. lutzii* was measured in 5 μg of protein extracts using the ab139435 PKA Activity Kinase Kit (Abcam, Cambridge, UK) following the manufacturer's guidelines. This kit is based on a solid phase enzyme-linked immuno-absorbent assay (ELISA). It uses a specific synthetic peptide as a substrate for PKA, and a polyclonal antibody that recognizes the phosphorylated form of the substrate.

3. Results

To investigate the physiological relevance of PKA on the morphological changes of *P. lutzii*, we examined the effects of the H89 in the mycelium to yeast transition.

3.1. Molecular modeling studies

Considering the absence of X-ray structures on the Protein Data Bank (PDB) database [43], homology models were built for *P. lutzii* PKA based on the following steps: (i) identification of structural templates in PDB, (ii) alignment of *P. lutzii* PKA sequence and template structures, (iii) model building, (iv) structure refinement, and (v) model quality evaluation. The best model was built using *Bos taurus* cAMP-dependent protein kinase, alpha-catalytic subunit, available under PDB code 1XH9 (resolution = 1.6 Å, sequence identity = 43%, and coverage = 75%). The 3D structure of the built PKA model is shown in Fig. 1.

Validation of the 3D model was done for various levels of structural organization. Analysis of structure revealed that only 0.3% of amino acids are within the disallowed Ramachandran and poor rotamer regions. On the other hand, 95.1% of amino acids are within the favored Ramachandran regions and have good rotamers, showing the good quality of the backbone dihedral angles (ψ against φ) and side-chain angles (χ) of amino acids. In addition, acceptable Clashscore (0.0) and MolProbity (0.84) scores were obtained for this structure. The Clashscore is the number of serious steric clashes per 1000 atoms. Already the MolProbity score is a log-weighted combination of the percentage of bad side-chain rotamers, the percentage of Ramachandran outliers, and the Clashscore, giving one number that reflects the resolution of X-ray structures at which those values would be expected [31]. Therefore, these overall characteristics suggest that the PKA model can be useful to prospective molecular modeling investigations.

Aiming to investigate the most energetically favorable interactions in the *P. lutzii* PKA surface, the homology model was applied to a hot spots analysis. This tool uses a detailed energy expression (including attractive and repulsive van der Waals terms, electrostatic interaction energy, desolvation energy, and a structure-based pairwise interaction potential) to sample probe positions (of small organic molecules) on the protein surface. In particular, the key protein residues and secondary structures that interact with bound probe molecules in the *P. lutzii* PKA structure are shown in Fig. 1B. To ensure that the hot spots were more recognizable, different colors were used to denote them according to the number of probe clusters that bind to them. The probe molecules (highlighted in gold) that bind to the ATP pocket interact with residues Lys129, Glu185, Asp225, Lys227, Glu229, Asn230, and Phe387, demonstrating the importance of these residues for accommodating small molecules. The probes also showed interactions with Val102, Thr104, and Thr106, Phe107, and Val110 of the P-loop (highlighted in magenta), and with Asp243 of the DGF-motif (highlighted in green).

To understand the affinity and intermolecular interactions of H89 with *P. lutzii* PKA, we performed molecular docking. The ChemGauss4 score (−11.2) suggests that H89 could inhibit *P. lutzii* PKA at low micromolar concentrations, as demonstrated in our experiments. In addition, analysis of poses showed that the predicted binding mode of H89 for *P. lutzii* PKA is similar to its experimental binding mode on mammalian PKAs (PDB accession number 1YDT) [44]. As we can see in Fig. 1C, isoquinoline moiety of the H89 inhibitor interacts with the hydrophobic pocket formed by Val110, Leu 178, Leu232, and Phe387, whereas the aromatic nitrogen forms a hydrogen bond interaction (represented as green dashed lines) with the main chain of Cys181. In addition, aliphatic amine forms a hydrogen bond interaction with the main chain of Glu228, whereas 4-bromobenzyl forms Van der Waals interactions with Phe107, Val110, and Lys129.

3.2. Effect of H89 on the morphological transition of *P. lutzii*

We analyzed the morphological transition in cultures treated with three different concentrations of H89: 25 μM, 50 μM (data not shown) and 100 μM. This initial evaluation showed that 100 μM H89 effectively

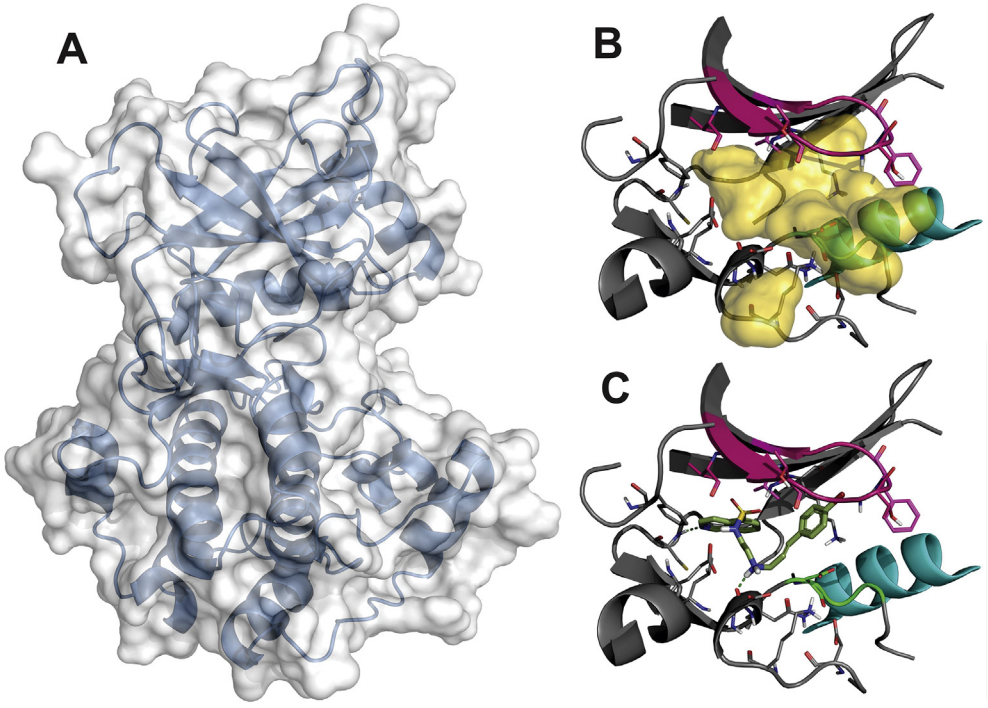

Fig. 1. Molecular modeling studies. (A) 3D structure of *P. lutzii* PKA homology model. (B) Hot spots analysis for the PKA model and (C) its intermolecular interactions with inhibitor H89. The hot spots are shown in gold. The P-loop, DFG motif, and helix αC are highlighted in magenta, green, and blue, respectively.

blocks cellular differentiation without killing the cells. As a result, all the experiments described below were done with 100 μM H89.

The morphological transition was blocked in the presence of H89, indicating that PKA plays an important role in this process. As depicted in Figs. 2A and B, in the control culture, mycelium was completely converted into the yeast form 72 h after induction of transition. On the other hand, cells treated with H89 failed to change morphology, except for a few yeast cells observed in the 72 h culture. Cell viability was evaluated to demonstrate that H89, at the concentration used in our experiments, did not cause cell death. As shown in Fig. 2C, the viability rate was above 80% in all the cultures, which is considered a good result for toxicity tests.

3.3. PKA activity increases during the mycelium to yeast transition

PKA activity increases significantly during the mycelium to yeast transition. We can observe a slow and gradual increase in activity in the first 48 h of differentiation and a sudden rise at 72 h. The activity of PKA is >5 times higher in protein extracts obtained from yeast cells than from mycelium. In contrast, in protein extracts from cells treated with H89, enzyme activity drops in the first 48 h of cell differentiation, although it rises discreetly at 72 h, as shown in Fig. 3.

Our results show a correlation between the mycelium to yeast transition and PKA activity in *P. lutzii*, confirming that PKA is essential for the cell differentiation process in this fungus.

3.4. P. lutzii recovers the ability to change morphology when H89 is removed from the culture media

We analyzed the ability of *P. lutzii* to resume differentiation after removing H89 from the culture. In this assay, cells were treated with H89 for 48 h, washed, transferred to fresh media without inhibitor, and then grown for another 48 h. Figs. 4A and B show that cells recover from H89 treatment and rapidly turn into yeast when the inhibitor is taken away (from 48 h to 96 h). Cell viability was monitored throughout the experiment and is almost 90% both for the control and treated cells (Fig. 4C).

As shown in Fig. 5, it is noteworthy that recovery is accompanied by an increase in PKA activity, reinforcing the relationship between PKA and phase transition in *P. lutzii*.

4. Discussion

Previous studies have established that the cAMP-signaling pathway is important in controlling the morphological transition in *P. brasiliensis* [25]. It has been shown that the Gβ protein Gpb1 and the TupA transcriptional co-regulator bind to the Tpk2 subunit of PKA in order to act as antagonistic molecular switches of *P. brasiliensis* morphological changes [26]. Therefore, in order to understand how PKA impacts dimorphism in *P. lutzii*, we used the PKA specific inhibitor H89. This strategy has been successfully used to analyze PKA activity in other fungi [45,46].

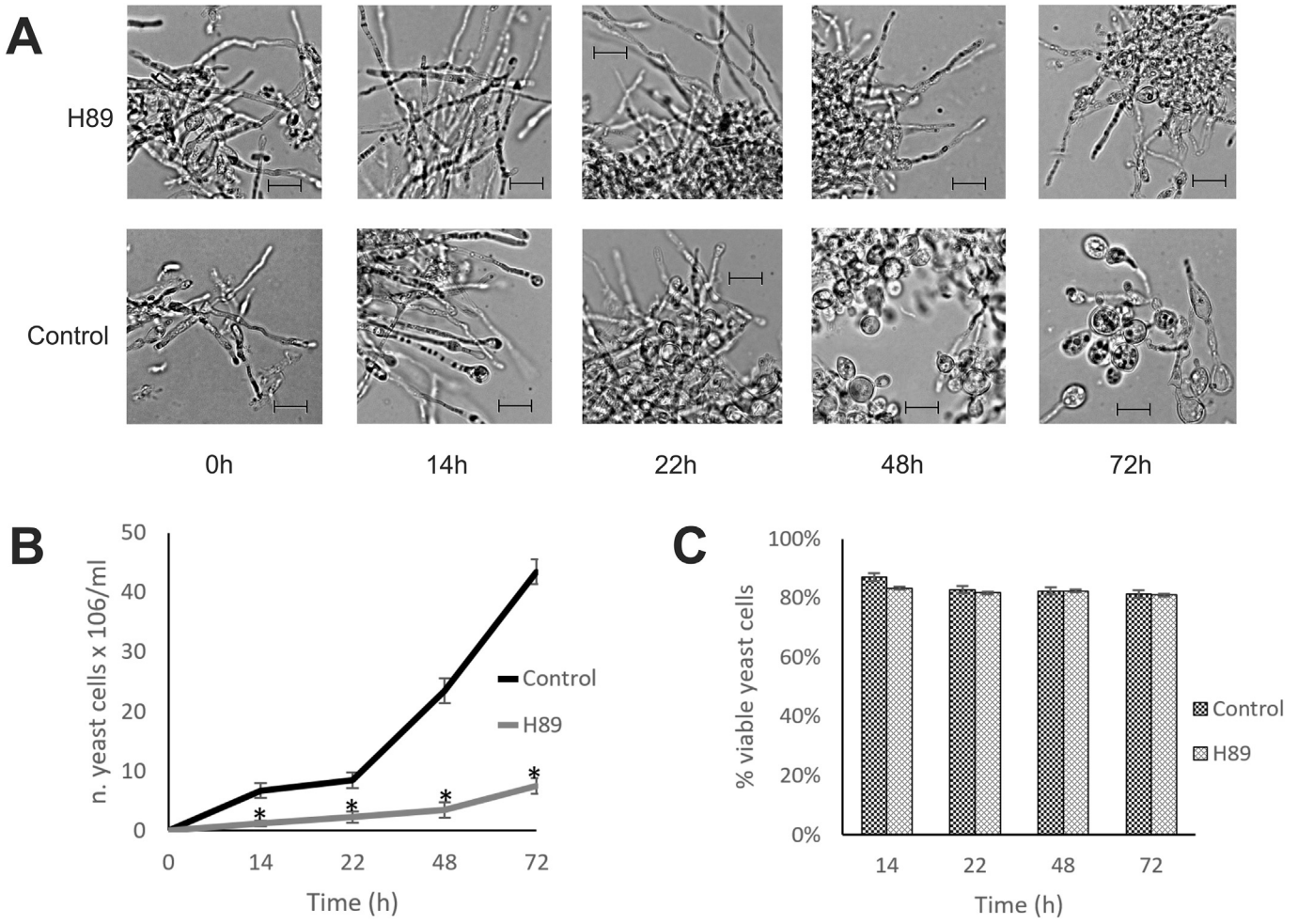

Fig. 2. Effect of H89 in the mycelium to yeast transition. (A) Comparative cellular morphology. Bars represent 10 μm. (B) Quantification of the number of yeast cells throughout phase transition. The mycelium to yeast transition was quantified in a Neubauer Chamber by counting the number of yeast cells that appeared in the culture medium after changing the incubation temperature from 22 °C to 36 °C. *Statistically significant data compared to the control. (C) Cell viability determined using trypan blue staining and standard cell count techniques.

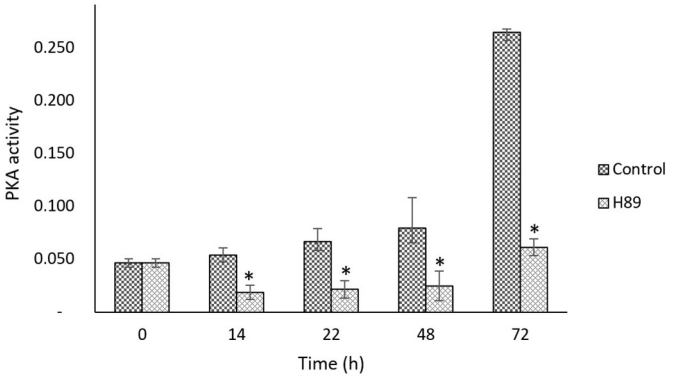

Fig. 3. PKA activity in *P. lutzii* protein extracts obtained during the mycelium to yeast transition. *Statistically significant data compared to the control ($p \leq 0.05$).

In this work, we show that H89, a molecular probe frequently used to inhibit kinase signaling pathways, may have *in vitro* activity against *P. lutzii* through inhibition of PKA. In order to elucidate the structural basis for inhibition and to enable structure-based drug design of potential therapeutic agents for treatment of paracoccidioidomycosis, molecular modeling studies were performed. The hot spots analysis showed important energetic contributions of the ATP-binding site residues for interaction with H89. Important hydrogen bond interactions between the enzyme and the ligand include the isoquinoline ring nitrogen with the backbone amide of Cys181 and aliphatic amine with the backbone carbonyl of Glu228. In addition, the *in silico* analysis revealed similar binding modes of H89 in fungal and mammalian PKAs, but different hydrophobicity of the two binding sites. Several amino acid residues of the binding site (Cys181, Val102 and Thr106) of *P. lutzii* PKA were substituted in mammalian PKAs by Val181, Leu102 and Ser106, respectively. These key differences between enzymes combined with hot spots analysis and binding mode of H89 may be useful to design more potent and selective antifungal drug candidates.

In this study, we focused on the mycelium to yeast transition since this is the process observed in nature and it is key to establishment of the infection. Our *in vitro* assays show that H89 blocks the dimorphic transition in *P. lutzii* by drastically reducing PKA activity. We demonstrate that PKA activity is phase regulated in *P. lutzii*, being about five

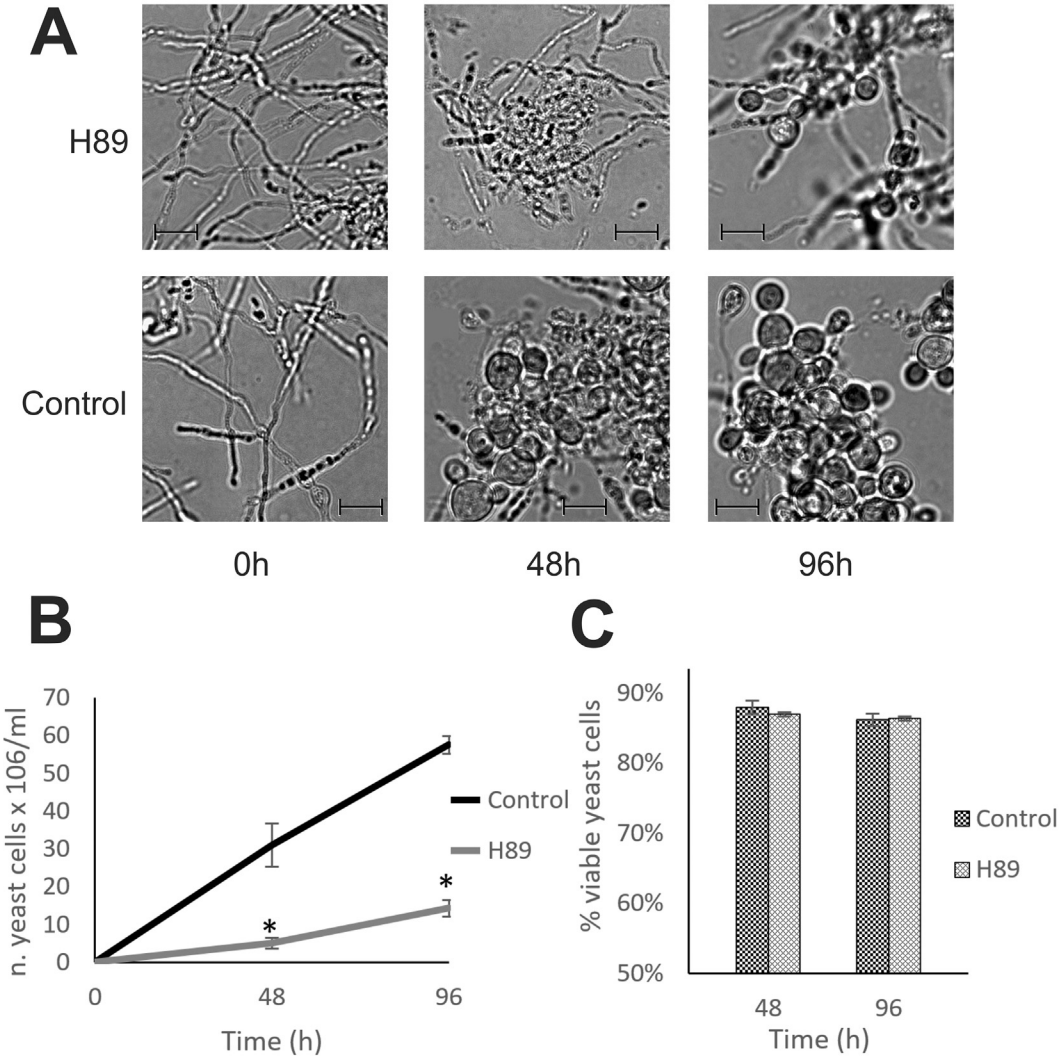

Fig. 4. Phase transition in cells treated with H89 for 48 h, and in cells recovering from treatment for an additional 48 h (in a 96 h assay). (A) Comparative cellular morphology. Bars represent 10 μm. (B) Quantification of the number of yeast cells throughout phase transition. The mycelium to yeast transition was quantified by counting the number of yeast cells that appeared in the culture medium after changing the incubation temperature from 22 °C to 36 °C. After 48 h of morphological transition, H89 treated cells were washed to remove the inhibitor, transferred to fresh liquid Fava Netto's medium without inhibitor and grown for additional 48 h (in a total of 96 h). *Statistically significant data compared to the control ($p \leq 0.05$). (C) Cell viability determined using trypan blue staining and standard cell count techniques.

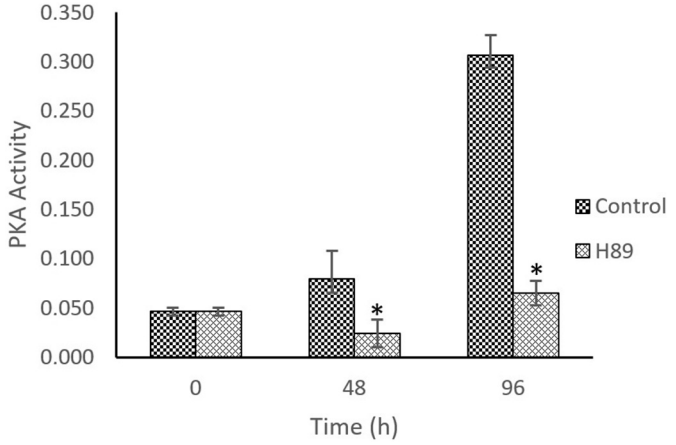

Fig. 5. PKA activity in protein extracts obtained from cells treated with H89 and during recovery from treatment. Protein extracts obtained at 48 h of morphological transition from H89 treated cells and from cells recovering from H89 treatment for additional 48 h (in a total of 96 h). *Statistically significant data compared to the control. Statistical analyses were evaluated by Student's test ($p \leq 0.05$).

times higher in protein extracts obtained from yeast cells when compared to mycelium. PKA activity is also correlated with morphogenesis in *S. cerevisiae*. In this organism, mutants with constitutively high PKA activity are hyperfilamentous; whereas those with low PKA activity cannot switch to the filamentous form [19,47].

As shown, the halt in phase transition is accompanied by a decrease in PKA activity. But the fungus resumes cell differentiation when the inhibitor is removed from the culture media, reinforcing the relationship between PKA activity and dimorphism in *P. lutzii*. H89 blocks PKA activity through a reversible competitive inhibition of the ATP site on the PKA catalytic subunit.

Although H89 is widely used in the study of PKA effects, this approach may have some inconveniences. The concentration of the drug required for effective protein kinase blockade varies according to the ATP concentration in the cell. Furthermore, although H89 is a specific PKA inhibitor, some studies have suggested that it also inhibits other kinases [48–50].

As shown here for *P. lutzii*, PKA contributes to the regulation of cell shape changes in other fungi, such as *S. cerevisiae*, *C. neoformans* and *C. albicans* [9–11,19,20]. In *C.albicans*, 100 μM H89 effectively blocks phase transition [45].

It is important to highlight that we evaluated cell viability during the assays to be sure that the block in phase transition is not due to death of the fungus, but rather as a result of PKA inhibition. The viability rate was above 80% in both the control and treated cultures.

5. Conclusion

Taken together, our results strongly support the importance of PKA with regard to *P. lutzii* dimorphism, demonstrating that the activity of this protein is essential for the mycelium to the pathogenic yeast transition in *P. lutzii*.

Acknowledgments

The authors thank Dr. A Walmsley and Dr. MI Borges-Walmsley from Durham University for the helpful discussions. We also are grateful to OpenEye Scientific Software Inc. (https://www.eyesopen.com/) for providing academic license of their software.

Funding

This work was supported by grants from Conselho Nacional de Desenvolvimento Científico e Tecnológico (CNPq Edital Universal 485084/2012-0). Sestari was supported by a fellowship from Coordenação de Aperfeiçoamento de Pessoal de Nível Superior (CAPES) (1579196).

References

[1] T. Hunter, Protein kinases and phosphatases: the Yin and Yang of protein phosphorylation and signaling, Cell 80 (1995) 225–236.
[2] T. Hunter, Signaling—2000 and beyond, Cell 100 (2000) 113–127.
[3] P. Cohen, Protein kinases—the major drug targets of the twenty-first century? Nat. Rev. Drug Discov. 1 (2002) 309–315.
[4] R.A. Engh, D. Bossemeyer, The protein kinase activity modulation sites: mechanism for cellular regulation - targets for therapeutic intervention, Adv. Enzym. Regul. 41 (2001) 121–149.
[5] G. Manning, The protein kinase complement of the human genome, Science 298 (2002) 1912–1934.
[6] D.R. Knighton, J.H. Zheng, L.F. Ten Eyck, V.A. Ashford, N.H. Xuong, S.S. Taylor, J.M. Sowadski, Crystal structure of the catalytic subunit of cyclic adenosine monophosphate-dependent protein kinase, Science 253 (1991) 407–414.
[7] S.K. Hanks, A.M. Quinn, T. Hunter, The protein kinase family: conserved features and deduced phylogeny of the catalytic domains, Science 241 (1988) 42–52.
[8] S.S. Taylor, C. Kim, C.Y. Cheng, S.H.J. Brown, J. Wu, Signaling Through cAMP and cAMP-dependent Protein Kinase: Diverse Strategies for Drug Design, 1784, 2008 16–26.
[9] C.R. Rocha, K. Schröppel, D. Harcus, A. Marcil, D. Dignard, B.N. Taylor, D.Y. Thomas, M. Whiteway, E. Leberer, Signaling through adenylyl cyclase is essential for hyphal growth and virulence in the pathogenic fungus *Candida albicans*, Mol. Biol. Cell 12 (2001) 3631–3643.
[10] W.H. Jung, L.I. Stateva, The cAMP phosphodiesterase encoded by CaPDE2 is required for hyphal development in *Candida albicans*, Microbiology 149 (2003) 2961–2976.
[11] J.A. Alspaugh, R. Pukkila-Worley, T. Harashima, L.M. Cavallo, D. Funnell, G.M. Cox, J.R. Perfect, J.W. Kronstad, J. Heitman, Adenylyl cyclase functions downstream of the Gα protein Gpa1 and controls mating and pathogenicity of *Cryptococcus neoformans*, Eukaryot. Cell 1 (2002) 75–84.
[12] B. Liebmann, S. Gattung, B. Jahn, A.A. Brakhage, cAMP signaling in *Aspergillus fumigatus* is involved in the regulation of the virulence gene pksP and in defense against killing by macrophages, Mol. Gen. Genomics. 269 (2003) 420–435.
[13] S. Gold, G. Duncan, K. Barrett, J. Kronstad, cAMP regulates morphogenesis in the fungal pathogen *Ustilago maydis*, Genes Dev. 8 (1994) 2805–2816.
[14] S.J. Klosterman, M.H. Perlin, M. Garcia-Pedrajas, S.F. Covert, S.E. Gold, Genetics of morphogenesis and pathogenic development of *Ustilago maydis*, Adv. Genet. 57 (2007) 1–47.
[15] W. Choi, R.A. Dean, The adenylate cyclase gene MAC1 of *Magnaporthe grisea* controls appressorium formation and other aspects of growth and development, Plant Cell 9 (1997) 1973–1983.
[16] H. Liu, A. Suresh, F.S. Willard, D.P. Siderovski, S. Lu, N.I. Naqvi, Rgs1 regulates multiple Gα subunits in *Magnaporthe pathogenesis*, asexual growth and thigmotropism, EMBO J. 26 (2007) 690–700.
[17] T. Toda, S. Cameron, P. Sass, M. Zoller, M. Wigler, Three different genes in *S. cerevisiae* encode the catalytic subunits of the cAMP-dependent protein kinase, Cell 50 (1987) 277–287.
[18] W.-S. Lo, A.M. Dranginis, The cell surface Flocculin Flo11 is required for Pseudohyphae formation and invasion by *Saccharomyces cerevisiae*, Mol. Biol. Cell 9 (1998) 161–171.
[19] X. Pan, J. Heitman, Cyclic AMP-dependent protein kinase regulates pseudohyphal differentiation in *Saccharomyces cerevisiae*, Mol. Cell. Biol. 19 (1999) 4874–4887.
[20] L.S. Robertson, G.R. Fink, The three yeast a kinases have specific signaling functions in pseudohyphal growth, Proc. Natl. Acad. Sci. U. S. A. 95 (1998) 13783–13787.
[21] C. De Moraes Borba, G.M.V. Schäffer, *Paracoccidioides brasiliensis*: virulence and an attempt to induce the dimorphic process with fetal calf serum, Mycoses 45 (2002) 174–179.
[22] J.C. Nemecek, Global control of dimorphism and virulence in fungi, Science 312 (2006) 583–588.
[23] A. Restrepo, J.G. McEwen, E. Castañeda, The habitat of *Paracoccidioides brasiliensis*: how far from solving the riddle? Med. Mycol. 39 (2001) 233–241.
[24] S. Paris, S. Duran, Cyclic adenosine 3′,5′ monophosphate (cAMP) and dimorphism in the pathogenic, Mycopathologia 92 (1985) 115–120.
[25] D. Chen, T.K. Janganan, G. Chen, E.R. Marques, M.R. Kress, G.H. Goldman, A.R. Walmsley, M.I. Borges-Walmsley, The cAMP pathway is important for controlling the morphological switch to the pathogenic yeast form of *Paracoccidioides brasiliensis*, Mol. Microbiol. 65 (2007) 761–779.
[26] T.K. Janganan, G. Chen, D. Chen, J.F. Menino, F. Rodrigues, M.I. Borges-Walmsley, A.R. Walmsley, A Gβ protein and the TupA co-regulator bind to protein kinase A Tpk2 to act as antagonistic molecular switches of fungal morphological changes, PLoS One 10 (2015) 1–28.
[27] R. Apweiler, UniProt: the universal protein knowledgebase, Nucleic Acids Res. 32 (2004) 115D–119D.
[28] M. Biasini, S. Bienert, A. Waterhouse, K. Arnold, G. Studer, T. Schmidt, F. Kiefer, T.G. Cassarino, M. Bertoni, L. Bordoli, T. Schwede, SWISS-MODEL: modelling protein tertiary and quaternary structure using evolutionary information, Nucleic Acids Res. 42 (2014) 252–258.
[29] L. Bordoli, F. Kiefer, K. Arnold, P. Benkert, J. Battey, T. Schwede, Protein structure homology modeling using SWISS-MODEL workspace, Nat. Protoc. 4 (2009) 1–13.
[30] J. Ko, H. Park, L. Heo, C. Seok, GalaxyWEB server for protein structure prediction and refinement, Nucleic Acids Res. 40 (2012) W294–W297.

[31] V.B. Chen, W.B. Arendall, J.J. Headd, D.A. Keedy, R.M. Immormino, G.J. Kapral, L.W. Murray, J.S. Richardson, D.C. Richardson, MolProbity: all-atom structure validation for macromolecular crystallography, Acta Crystallogr., Sect. D: Biol. Crystallogr. 66 (2010) 12–21.
[32] D. Kozakov, L.E. Grove, D.R. Hall, T. Bohnuud, S.E. Mottarella, L. Luo, B. Xia, D. Beglov, S. Vajda, The FTMap family of web servers for determining and characterizing ligand-binding hot spots of proteins, Nat. Protoc. 10 (2015) 733–755.
[33] C.H. Ngan, T. Bohnuud, S.E. Mottarella, D. Beglov, E.A. Villar, D.R. Hall, D. Kozakov, S. Vajda, FTMAP: extended protein mapping with user-selected probe molecules, Nucleic Acids Res. 40 (2012) 271–275.
[34] OMEGA v.2.5.1: OpenEye Scientific Software, Santa Fe, NM. http://www.eyesopen.com., (n.d.).
[35] P.C.D. Hawkins, A.G. Skillman, G.L. Warren, B.A. Ellingson, M.T. Stahl, Conformer generation with OMEGA: algorithm and validation using high quality structures from the protein databank and Cambridge structural database, J. Chem. Inf. Model. 50 (2010) 572–584.
[36] A. Jakalian, D.B. Jack, C.I. Bayly, Fast, efficient generation of high-quality atomic charges. AM1-BCC model: II. Parameterization and validation, J. Comput. Chem. 23 (2002) 1623–1641.
[37] QUACPAC v.1.6.3: OpenEye Scientific Software, Santa Fe, NM. http://www.eyesopen.com., (n.d.).
[38] C.R. Søndergaard, M.H.M. Olsson, M. Rostkowski, J.H. Jensen, Improved treatment of ligands and coupling effects in empirical calculation and rationalization of pKa values, J. Chem. Theory Comput. 7 (2011) 2284–2295.
[39] J.L. Banks, H.S. Beard, Y. Cao, A.E. Cho, W. Damm, R. Farid, A.K. Felts, T.A. Halgren, D.T. Mainz, J.R. Maple, R. Murphy, D.M. Philipp, M.P. Repasky, L.Y. Zhang, B.J. Berne, R.A. Friesner, E. Gallicchio, R.M. Levy, Integrated modeling program, applied chemical theory (IMPACT), J. Comput. Chem. 26 (2005) 1752–1780.
[40] M. McGann, FRED pose prediction and virtual screening accuracy, J. Chem. Inf. Model. 51 (2011) 578–596.
[41] M. McGann, FRED and HYBRID docking performance on standardized datasets, J. Comput. Aided Mol. Des. 26 (2012) 897–906.
[42] OEDocking v.3.2.0: OpenEye Scientific Software, Santa Fe, NM. http://www.eyesopen.com., (n.d.).
[43] P.W. Rose, A. Prlić, C. Bi, W.F. Bluhm, C.H. Christie, S. Dutta, R.K. Green, D.S. Goodsell, J.D. Westbrook, J. Woo, J. Young, C. Zardecki, H.M. Berman, P.E. Bourne, S.K. Burley, The RCSB Protein Data Bank: views of structural biology for basic and applied research and education, Nucleic Acids Res. 43 (2015) D345–D356.
[44] R.A. Engh, A. Girod, V. Kinzel, R. Huber, D. Bossemeyer, Crystal structures of catalytic subunit of cAMP-dependent protein kinase in complex with isoquinolinesulfonyl protein kinase inhibitors H7, H8, and H89. Structural implications for selectivity, J. Biol. Chem. 271 (1996) 26157–26164.
[45] R. Castilla, S. Passeron, M.L. Cantore, *N*-Acetyl-D-glucosamine induces germination in *Candida albicans* through a mechanism sensitive to inhibitors of cAMP-dependent protein kinase, Cell. Signal. 10 (1998) 713–719.
[46] J.M. Mouillon, B.L. Persson, Inhibition of the protein kinase A alters the degradation of the high-affinity phosphate transporter Pho84 in *Saccharomyces cerevisiae*, Curr. Genet. 48 (2005) 226–234.
[47] S. Cameron, L. Levin, M. Zoller, M. Wigler, cAMP-independent control of sporulation, glycogen metabolism, and heat shock resistance in *S. cerevisiae*, Cell 53 (1988) 555–566.
[48] S.P. Davies, H. Reddy, M. Caivano, P. Cohen, Specificity and mechanism of action of some commonly used protein kinase inhibitors, Biochem. J. 351 (2000) 95–105.
[49] J. Bain, L. Plater, M. Elliott, N. Shpiro, C.J. Hastie, H. McLauchlan, I. Klevernic, J.S. Arthur, D.R. Alessi, P. Cohen, The selectivity of protein kinase inhibitors: a further update, Biochem. J. 408 (2007) 297–315.
[50] A. Lochner, J.A. Moolman, The many faces of H89: a review, Cardiovasc. Drug Rev. 24 (2006) 261–274.